Investigation of the Oven Process in Indirect Metal Laser Sintering

M. Seefried, M. F. Zaeh

iwb Institute for Machine Tools and Industrial Management, Technische Universitaet Muenchen, Germany

Abstract:

This paper deals with the optimization of Indirect Metal Laser Sintering. Different experimental analyses have proven that the oven process is highly responsible for the part distortion. By means of polished micrograph sections and thermogravimetric and dilatometric investigations, the oven process has been divided into four main steps: polymer removal, solid-state sintering, infiltration and liquid-phase sintering.
Further experiments were carried out at higher temperature phases of the oven process, using modified process parameters.
The aim of this research is to improve the knowledge about the oven process. In another step, this process will be simulated by means of finite element analysis in order to minimize the part distortion.

Introduction

Indirect Metal Laser Sintering is a manufacturing process that builds metal components layer by layer (fig. 1).
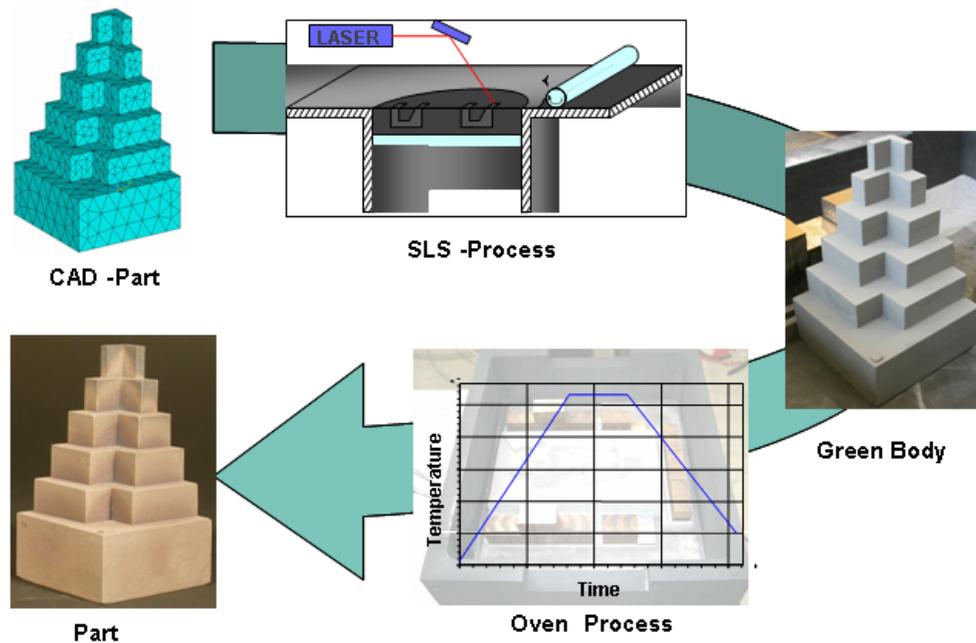
Fig. 1: Process flow of Indirect Metal Laser Sintering

All additive technologies are based on 3D-CAD solids. The first process step of Indirect Metal Laser Sintering is Selective Laser Sintering. The raw material is stainless steel that is powder coated by a PMMA-based polymer. The Selective Laser Sintering process works as follows:

The primary powder layer is applied to the building platform by an application mechanism. A CO_2-laser melts the polymer coating and the steel powder is thereby agglutinated to the layer geometry. This process is repeated until the whole component is completed. Because of the low rigidity of the produced parts, a heat treatment is needed. For this purpose, a special heat pattern is applied. The program raises the temperature up to 1070°C with a heating rate of 2 Kelvin/minute. After 3 hours at 1070°C, the temperature is cooled down at the same rate of 2 Kelvin/minute. Fig. 2 shows the temperature program used for the heat treatment in an oven.
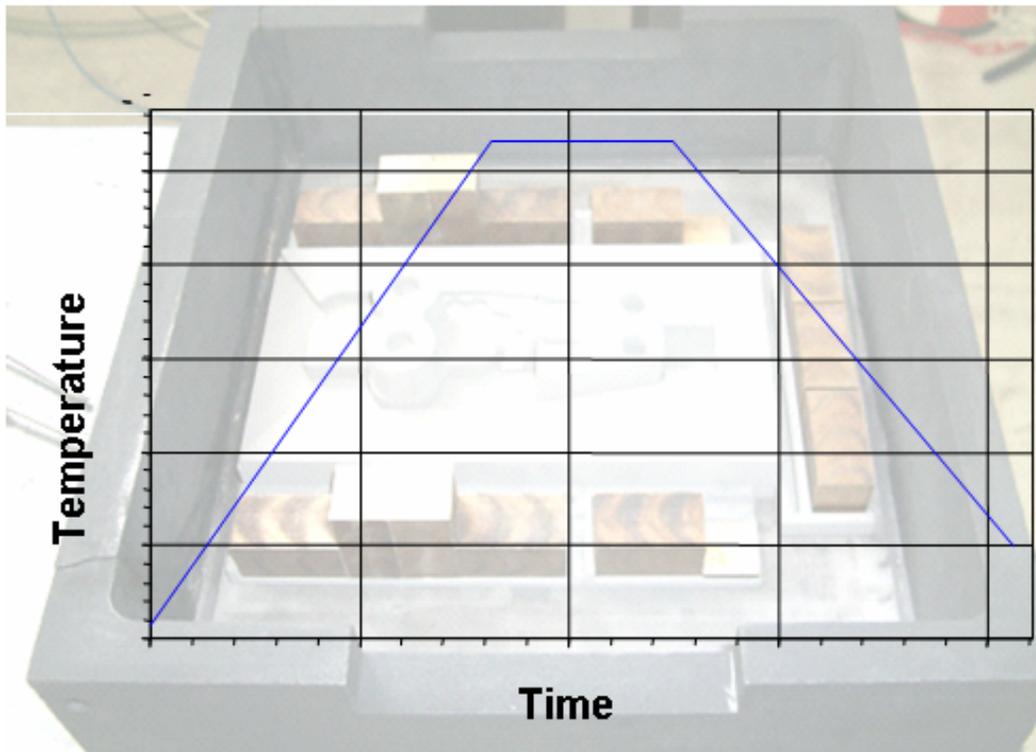
Fig. 2: Temperature program for heat treatment in the oven process

The resulting weight proportion of the product is 60 % stainless steel and 40 % bronze.

State of the art

The literature offers different approaches for developing and optimizing Indirect Metal Laser sintering. The main research is focused on selective Laser sintering and its consequences for the following oven process. These investigations were decisive for the development of the process [1; 2]. Other studies deal with the oven process, especially the process step of polymer removal [3; 4]. The aim of the research was to optimize parameter settings to prevent possible damage to the parts. In [5; 6; 7; 8] further fields of application for Indirect Metal Laser Sintering are discussed.

Fährer [9] describes an approach for integral optimization of the oven process for Indirect Metal Laser sintering by widening the system boundaries.

The aim of the presented research is to clarify the physical and chemical processes in order to optimize Indirect Metal Laser Sintering through finite element analysis. The entire research is based on a heuristic approach. The chronological order of the occurring processes and their physical characteristics has to be known and represented with different methods.

Classification of the process steps of polymer removal and infiltration

Fig. 2 shows the temperature as a control variable for the heat in the oven process. However, this does not allow any conclusions about the course of the heat within the part. The temperature serves as a reference for classifying further investigations, as for example thermal analysis.

The course of the heat within the parts has been determined by temperature measurements in different test series. Test items were positioned in a pan and covered with aluminum oxide powder in the oven, which was supplied by the Lindbergh Company. Several preliminary tests showed considerable heat traces from heat conduction between the ceramic plate in the graphite pan and the part positioned on top of it. Thus it became essential to use a part that did not have full contact with the bottom plate but had enough strength to hold the thermocouples. The test arrangement is shown in Fig. 3.

Fig. 3: Test item, thermocouples and test arrangement in the pan covered with aluminum oxide powder.

Fig. 4 shows the corresponding temperature course of the measurement.
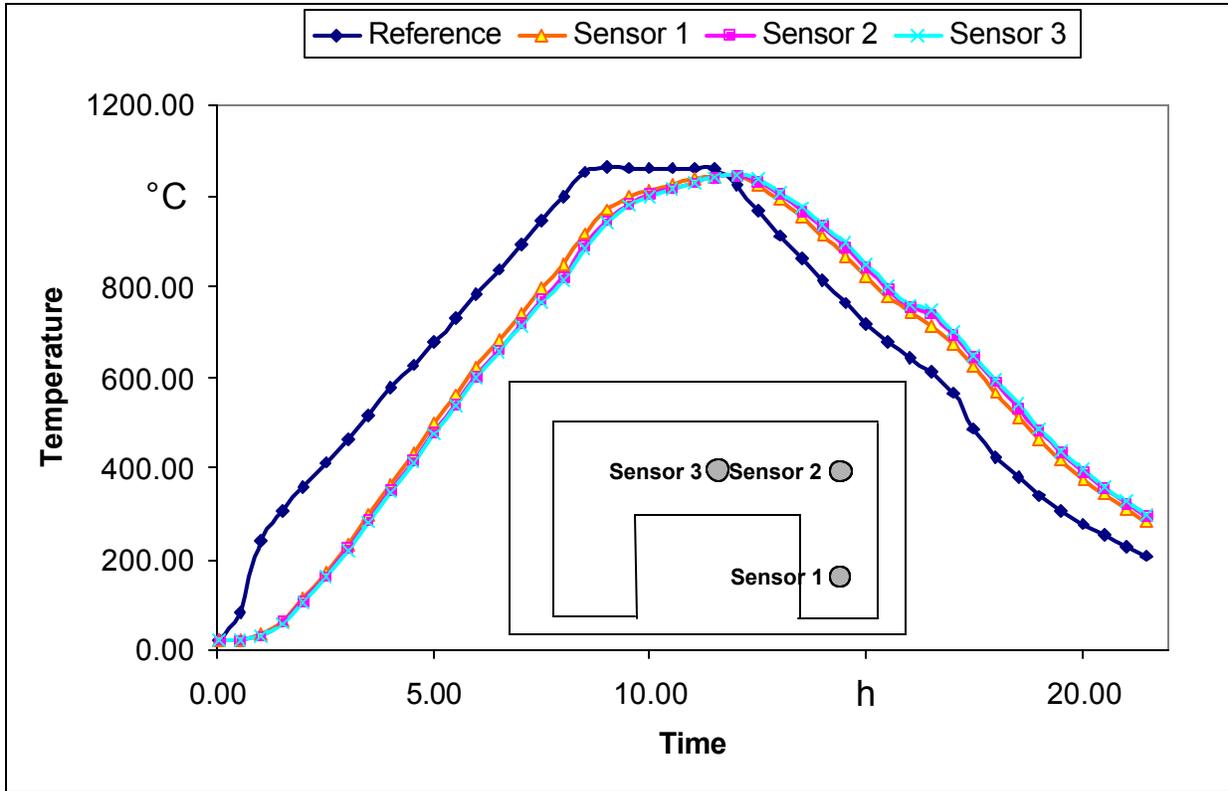
Fig. 4: Temperature course in the test item

The control signal for the oven is the reference temperature. It approximately corresponds to the temperature course during the heat treatment. For a better overview, Fig. 4 only shows the results of the temperature measurement of three sensors. The temperature course inside the test item varies from the reference temperature. Knowledge about the heat condition is important for coordinating chemical and physical processes. To classify the processes within the heat cycle, further investigations are necessary.

Thermogravimetry is a thermal analysis method for recording the mass loss over time. The results of a thermogravimetric measurement of a LaserForm ST-100 test part are shown in Fig. 4.

627
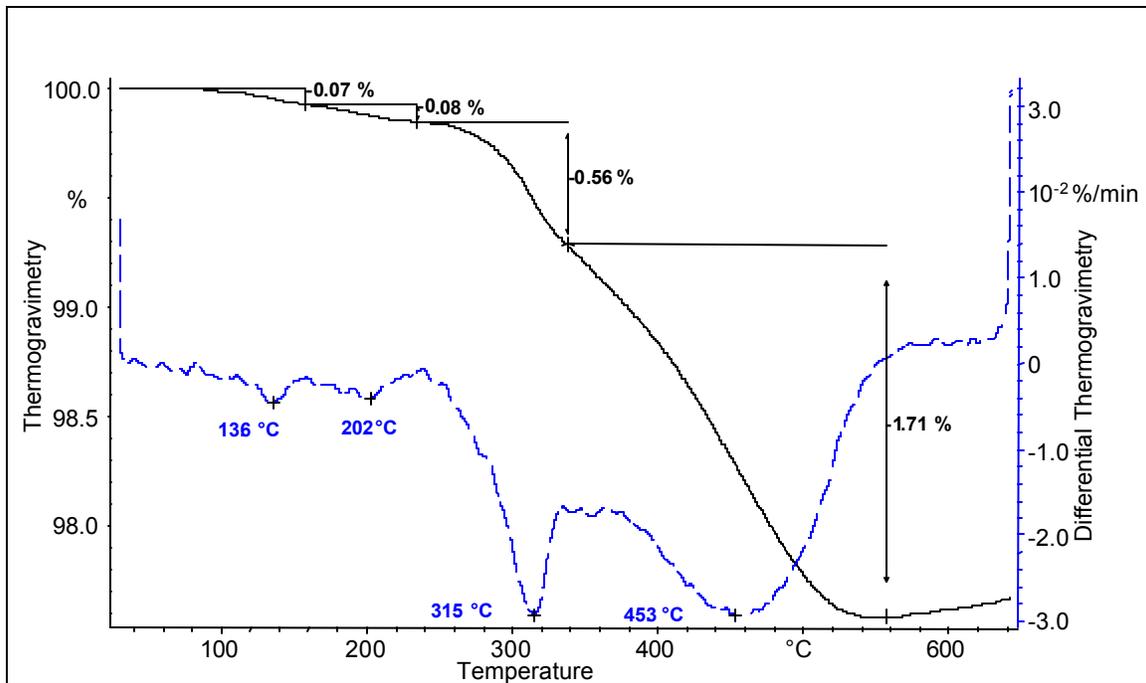
Fig. 5: Thermogravimetry of a green body

The mass loss approximately corresponds to the polymer removal. The polymer gasifies and diffuses out of the part. The decomposition begins at about 100°C. The main conversion takes place between 280°C and 540°C. Above 540° the conversion is finished and 2.4 weight percent is removed from the green body.

The process step of polymer removal therefore takes place at a temperature between 100°C and 540°C.

Different tests are necessary to estimate the temporal course during infiltration (Fig. 6). The temperature program was modified for this purpose: the heating and cooling down rates remained the same, but the maximal temperature and the duration of the holding temperature were changed. Fig. 6 shows the essential results based on the produced parts.
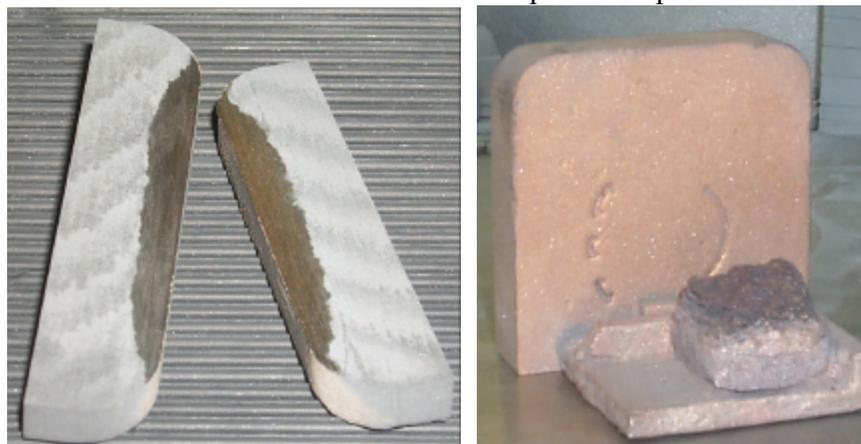
Fig. 6: Infiltration stopped at 1070°C after 1 h (partial infiltration and bronze flowing front) and after 1.5 h (full infiltration)

628

The part in the left picture (Fig. 6) was produced by stopping the infiltration at 1070°C after 1 h and subsequently cooling down. The infiltration is clearly distinguishable, but the progress of the infiltration is relatively low, although a flowing front can be seen.

The part in the right picture was produced by stopping the infiltration after 1.5 h. The infiltration is completely finished. The remaining infiltration material roughly corresponds to that of the conventional process.

This investigation demonstrates the following:

1. The infiltration process takes place over a time of approx. 30 min.
2. A flowing front of the infiltration material is developed.

Fig. 7 visualizes previous results of the temporal course of the process steps of polymer removal and infiltration, based on the determined real temperature course during the heat treatment.
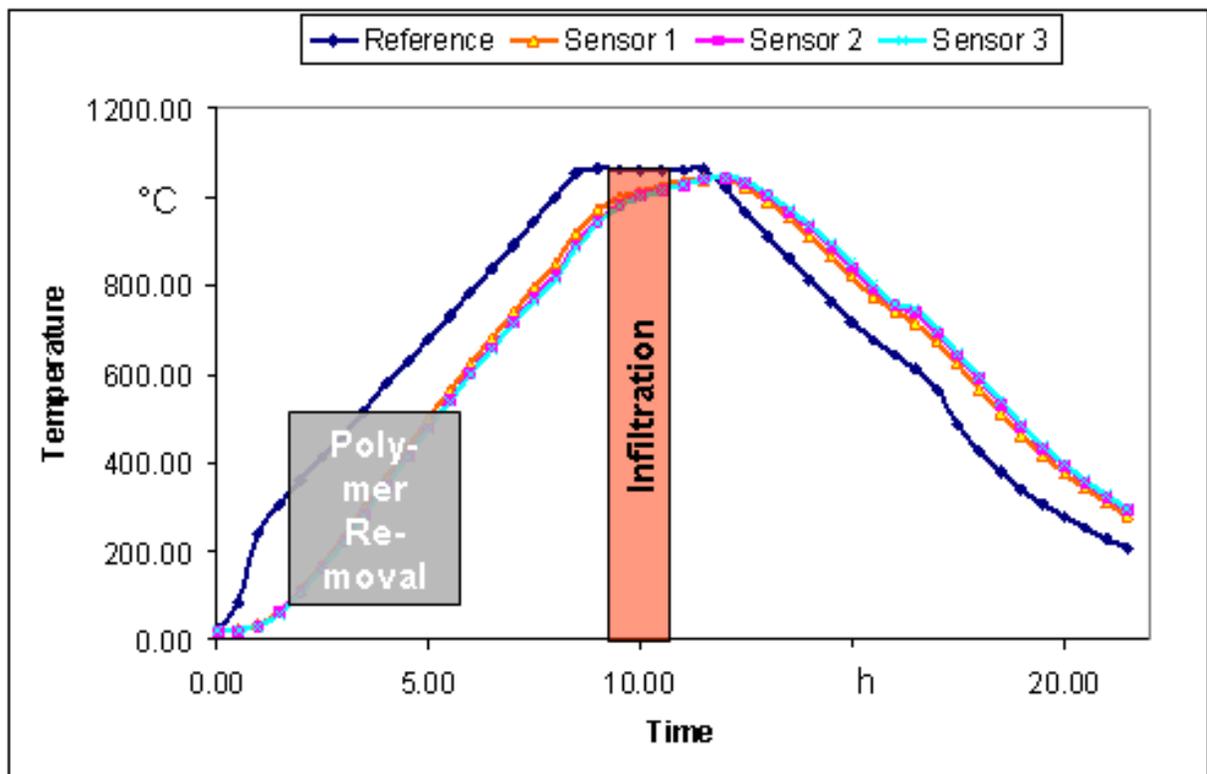
Fig. 7: Visualization of the temperature course during the heat treatment in the oven process and classification of the process steps of polymer removal and infiltration

Sintering

To clarify the physical processes between the process steps of polymer removal and infiltration, further tests were necessary. For this purpose, heat treatments were carried out with

629

modified temperatures during the oven process. Polished specimens were produced, which are presented in Fig. 8.
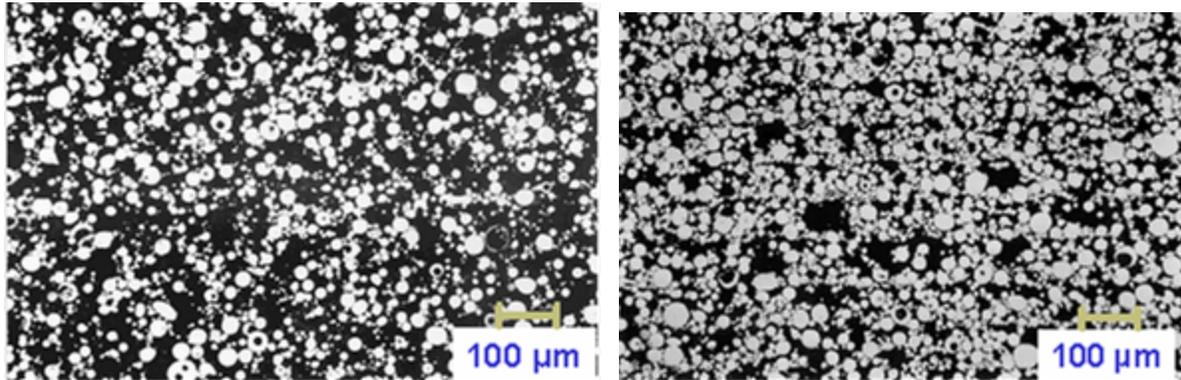
Fig. 8: Polished specimens of test items from temperature programs up to 600°C and 1070°C after 1 h

Fig. 8 shows micrographs of test items with different heat treatments. Heating and cooling down rates of 2 Kelvin/minute and 600°C maximal temperature affected the test item in the left picture. Light areas illustrate metal; dark areas illustrate blank spaces within the material. Isolated sintering necks among the metal particles indicate a very low degree of sintering. Generally, the part strength is low, which also explains the small number of metal particles compared to the voids. When micrographs are created, a sample has to be taken first. The top side is lapped, which can detach whole particles from samples with a low strength. Compared to the actual number, fewer metal particles will be seen on the micrograph because of the weak bonding forces.

The right side of Fig. 8 shows the micrograph of a sample after a heat treatment up to 1070°C for 1 h. The appearance of sintering necks can be observed. The strength properties of the material are determined by the sintering degree. According to German [10], this can be considered an early sintering stage.

The strength of the part is considerably higher than that of the previous one, and the number of metal particles is also much higher. Nevertheless, the removal of single particles from the compound can still be observed. Thus fewer particles remain on the lapped surface than there would normally be. In particular the larger black areas on the micrograph indicate torn-out particles.

Based on these insights, solid-state sintering takes place between the steps of polymer removal and infiltration. Particles are held together by friction forces before sintering necks are formed. The infiltration begins after the maximal temperature has been kept at 1070°C for one hour. At this point, molten bronze is absorbed because of the capillary forces in the porous material. The infiltration lasts for about 30 min. (Fig. 6). Areas not being infiltrated with bronze continue to sinter. The progress of the sintering is very little due to the short infiltration time and can be neglected in further investigations.

During infiltration, a second material is added to the part. A bronze phase develops at the edge and the part therefore swells; this is shown in Fig. 9.
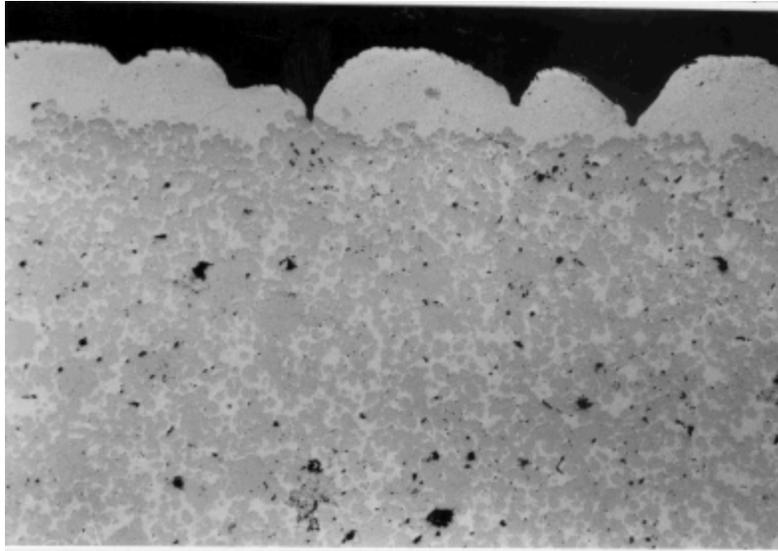
Fig. 9: Micrograph of a border area of an infiltrated sample.

In addition, the whole part swells as a consequence of the infiltration.

After infiltration, the part has a liquid phase and partially sintered stainless steel particles. This leads to the formation of inter-metallic phases, as shown by Breitinger [5].

The infiltration during the conventional temperature program is finished after 1.5 h at 1070°C. However, only 50 % of the heat treatment is finished at this time. In order to understand the remaining physical processes, it is necessary to observe the basic principles of the liquid-phase sintering.

As German [10] postulates, the requirements of liquid-phase sintering are:

- the existence of a liquid phase
- partial solubility of the solid in the liquid phase
- good wetting of the solid phase with the liquid phase
- diffusion of the solid phase into the liquid phase

When the iron/copper diagram and the iron/tin diagram are taken into account, it becomes evident that these requirements are met for the materials. Liquid-state sintering therefore takes place during the further heat treatment.

German [10] characterizes the liquid-phase sintering as shown in Fig. 10:

631

densification, %

sintering time, min
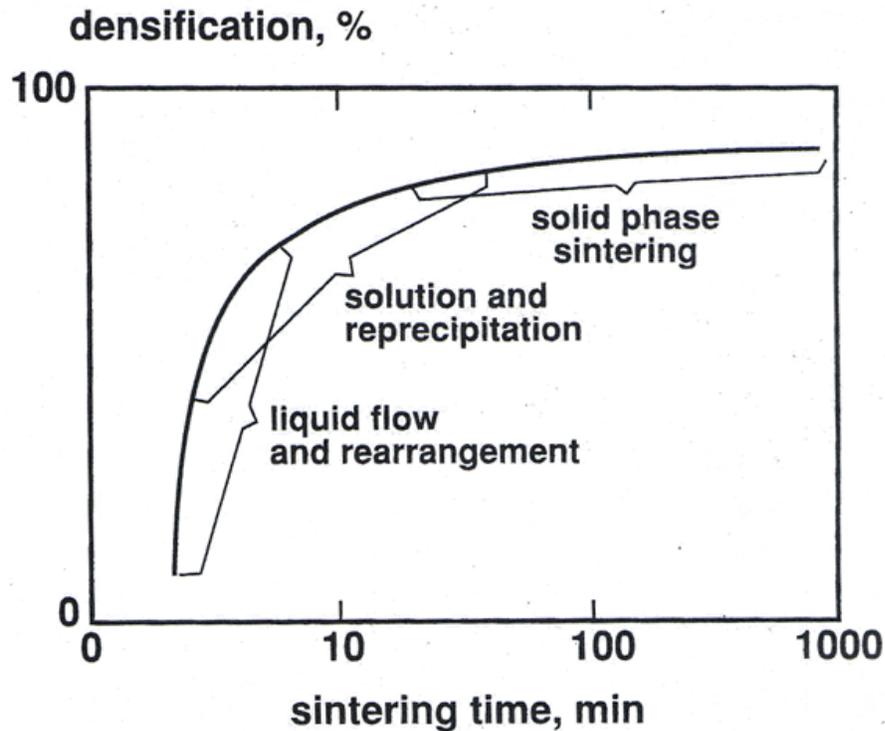
Fig. 10: Characterization of liquid-phase sintering [10]

Liquid-phase sintering can be divided into three density states:
- liquid flow and rearrangement
- solution and reprecipitation
- solid-phase sintering

The driving force in all sintering processes, as in liquid-phase sintering, is the reduction of the system surface energy.

The first two sintering states are decisively influenced by the liquid phase. This is when the greatest part of the densification and shrinkage takes place. Particles are rearranged according to the degree that the solid phase is wetted by the liquid phase. Good wetting leads to a reduction in friction among the particles and thus to a considerable rearrangement and densification. The very good ability of stainless steel to be wetted by bronze means that a considerable densification and shrinkage are to be expected. The time period of the particle rearrangement is relatively small. The solution, reprecipitation and solid-phase sintering can be neglected as far as the rearrangement of particles related to densification and shrinkage is concerned.

If one observes the thermal expansion coefficient during infiltration dilatometry (Fig. 10), the following becomes apparent above 1000°C: first the thermal expansion coefficient (alpha) increases because of the infiltration and the bronze phase formation at the border area. Then the liquid-phase sintering follows with the particle rearrangement as a considerable part of the entire shrinkage. The dilatometry reveals an alpha decrease in a temperature range of approximately

632

40°C, which corresponds to a time period of 16 minutes at a heating rate of approximately 2 Kelvin/minute. This represents a very good conformance between the theory of liquid phase sintering and measurements.
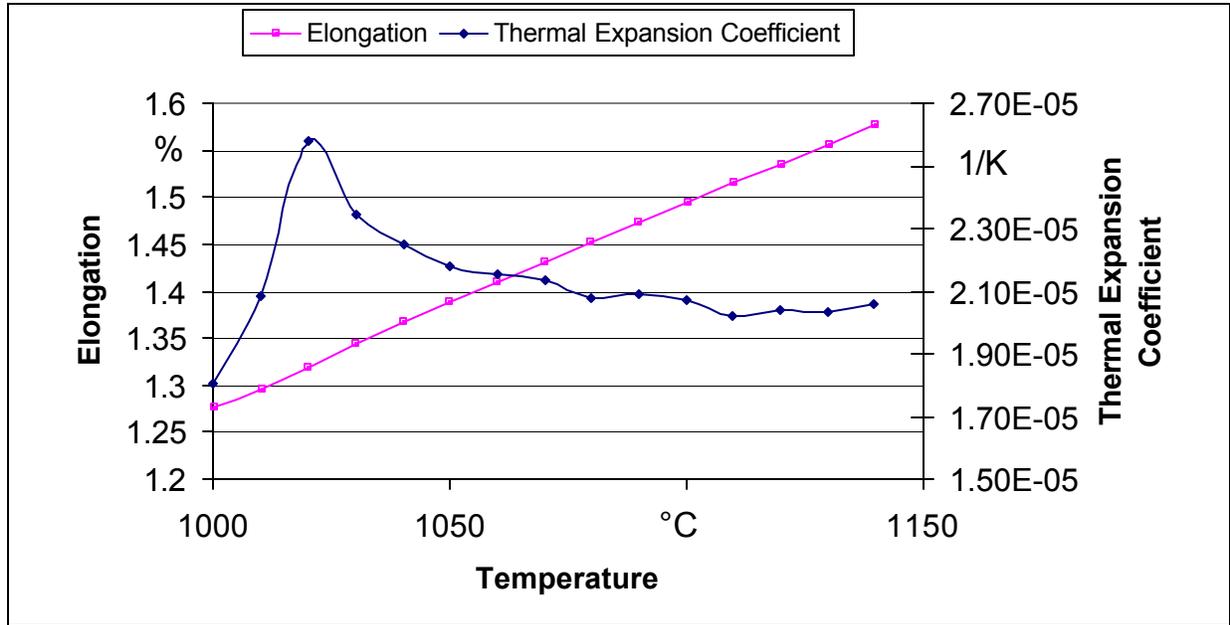
Fig. 10: Thermal expansion coefficient (alpha) between 1000 °C and 1150 °C

All previous facts suggest a liquid-phase sintering after infiltration. This takes place until the molten bronze solidifies at 798 °C [11]. Until this point in the cooling down period, the liquid phase sintering is verifiable. To determine the real time of solidification, it is necessary to consider the temperature within the part, which differs from the temperature as a controlling parameter of the oven as shown in Fig. 4. The solidification temperature is reached within the part after approximately 15 hours. Thus the liquid-phase sintering takes approximately 5 hours.

633

The whole process:

Based on all previous investigation results, Indirect Metal Laser Sintering can be presented as follows (fig. 11):
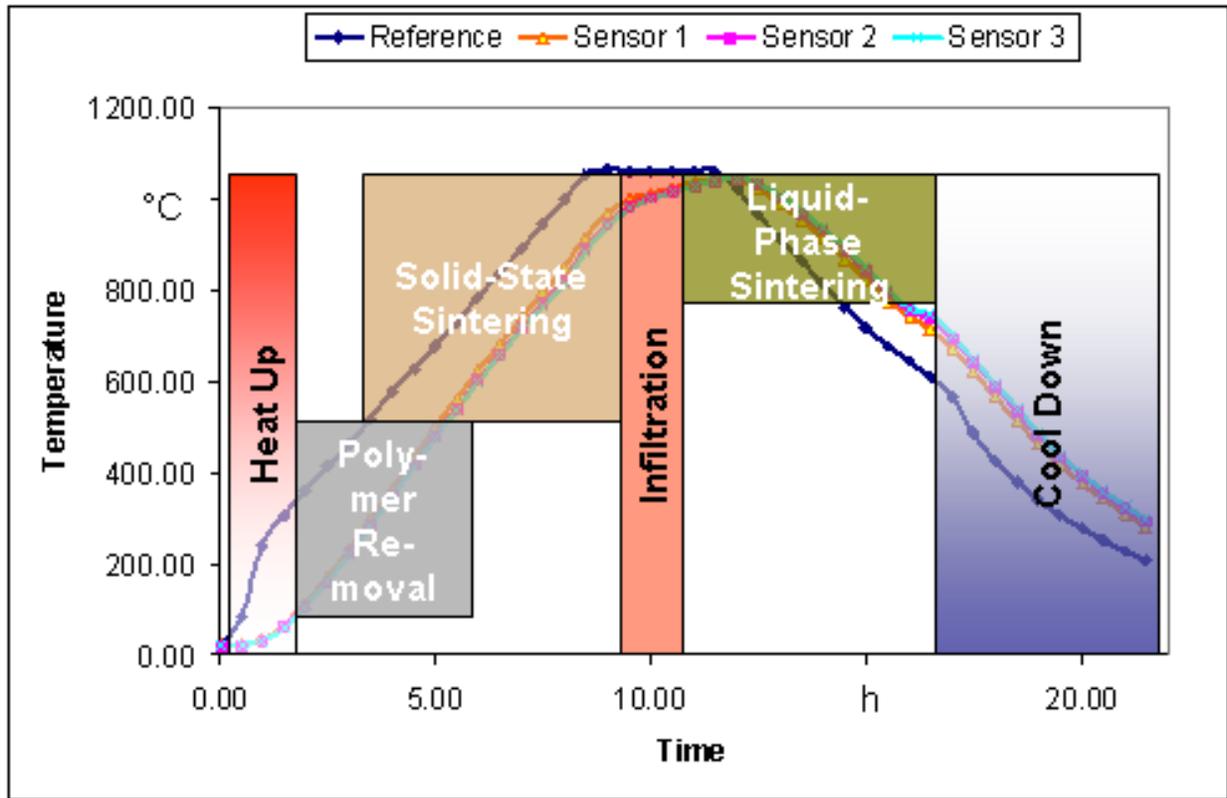
Fig. 11: Physical processes during heat treatment with Indirect Metal Laser Sintering

Perspectives

The present work investigates the physical processes during the heat treatment of green bodies to produce metallic parts with Indirect Metal Laser Sintering. This will serve as a basis for further development to enhance the precision of the whole process. Further studies will deal with creating separate simulation models for all processes during heat treatment.

The long-term aim of all studies is to create a simulation model for the whole process of Indirect Metal Laser Sintering. On the one hand, simulation models are used to determine and compensate distortions by means of an adjusted process chain before machining. On the other hand, special simulation models are to be developed for critical process steps, such as polymer removal, to optimize strength and surface quality.

References:

[1] Badrinarayn, B.; Barlow, J.W.: Effect of Processing Parameter in SLS of Metal-Polymer Powders. In: Solid Freeform Fabrication Symposium Proceedings. Texas: 1995, pp. 55-63.

634

[2] Vail, N. K.: Preparation and Characterization of Microencapsulated, Finely Divided Ceramic Materials for Selective Laser Sintering. Dissertation, University of Texas at Austin 1994.

[3] Beaman, J.; Barlow, J., W.; Bourell, D.; Crawford, R.: Solid Freeform Fabrication. A New Direction in Rapid Manufacturing. Dordrecht: Kluwer Academic Publishers 1997.

[4] Meindl, M.: Methoden zur Qualifizierung generativer Fertigungsverfahren für das Rapid Manufacturing. Dissertation, Technische Universitaet Muenchen 2004 (publication follows).

[5] Breitinger, F.: Ein ganzheitliches Konzept zum Einsatz des Indirekten-Metall-Lasersinterns für das Druckgießen. Dissertation, Technische Universitaet Muenchen 2002.

[6] Breitinger, F.; Lorenzen, J.: Rapid Tooling ein neuer Ansatz zur integrierten Produkt- und Prozessentwicklung. In: Rreinhart, G.; Milberg, J.: Rapid Tooling, Mit neuen Technologien schnell vom Entwurf zum Serienprodukt. Munich: Herbert Utz 1997

[7] Kühnle, H.; Stettin, A.: Stand und Potenzial lasergesinterter Druckgusswerkzeuge. Giesserei-Erfahrungsaustausch (1999) 7/8, pp. 433-437.

[8] Kühnle, H.; Stettin, A.; Hartmann, A.: Generative Fertigungsverfahren – eine Alternative für den Formenbau ?. Gießerei-Praxis (1999) 10, pp. 491-495.

[9] Fährer, J.: Ganzheitliche Optimierung des Indirekten-Metall-Lasersinterprozesses. Dissertation, Technische Universitaet Muenchen 2001.

[10] German, R.: Sintering Theory and Practice. New York: John Wiley & Sons 1996.

[11] Dies, K.: Kupfer und Kupferlegierungen in der Technik. Berlin: Springer 1967, p. 505.